Original Article

Both silicalite-1/SiC foam and ZSM-5/SiC foam may serve as novel bone replacement materials

Fengyu Hao[1], Cuicui Zhang[2], Lin Wu[2], Yong Gao[3], Yilai Jiao[3]

[1]Department of Dental Materials, [2]Department of Prosthodontics, School of Stomatology, China Medical University, Shenyang 110001, China; [3]Institute of Metal Research, Chinese Academy of Sciences, Shenyang 110016, China

Contributions: (I) Conception and design: L Wu; (II) Administrative support: F Hao, L Wu; (III) Provision of study materials or patients: Y Gao, Y Jiao; (IV) Collection and assembly of data: C Zhang; (V) Data analysis and interpretation: F Hao; (VI) Manuscript writing: All authors; (VII) Final approval of manuscript: All authors.

Correspondence to: Lin Wu, PhD. Department of Prosthodontics, School of Stomatology, China Medical University, No. 117, North Nanjing Street, Heping District, Shenyang 110001, China. Email: wulin13@163.com.

Background: This study aimed to analyze the bioactivity and biocompatibility of silicon carbide (SiC) foam coated with one of two kinds of zeolite.

Methods: The surface charges, protein adsorption ability and mineralization ability were compared between silicalite-1/SiC foam and ZSM-5/SiC foam.

Results: Proliferation and differentiation of primary osteoblasts seeded on two types of materials were significantly higher when compared with uncoated SiC foam after 7 d. There was no significant difference in the bioactivity between silicalite-1/SiC foam and ZSM-5/SiC foam. Silicalite-1/SiC foam and ZSM-5/SiC foam had no cytotoxic effect on primary osteoblasts.

Conclusions: These results suggest both silicalite-1/SiC foam and ZSM-5/SiC foam have the potential for use as novel bone replacement materials.

Keywords: Zeolite; silicon carbide (SiC); bioactivity; bone replacement material

Submitted Dec 08, 2018. Accepted for publication Apr 30, 2019.

doi: 10.21037/atm.2019.05.06

View this article at: http://dx.doi.org/10.21037/atm.2019.05.06

Introduction

A variety of people world wide suffer from bone defects and dysfunction caused by trauma, inflammation or bone tumors annually. A large quantity of orthopedic materials is needed to reconstruct the anatomical structure and restore the stability of the bone. In clinical practice, bone defects can be repaired with autograft or allograft materials. Nonetheless, these grafts have several disadvantages, including an inadequate supply, risk of disease transmission and unfavorable immune response. Thus, it is imperative to develop new bone replacement materials (1).

Silicon carbide (SiC) is a chemically inert ceramic material and is well known for its high biocompatibility. SiC ceramics have attracted a lot of interest in the field of biomedical devices and applications (2-5). Our *in vitro* and *in vivo* studies revealed SiC foam materials had favorable biological safety, good osteoconductivity, and osteogenic properties, which are almost equivalent to those of hydroxyapatite (HA) (6-8). Although SiC foam has stable physical and chemical performances, proper mechanical strength (compression strength ≥30 MPa, and elastic modulus between 20 and 30 GPa at 70% porosity with 1,000 μm pore size), and a controllable three-dimensional microstructure that matches bone, SiC foam is inert. How to improve the surface activity of SiC, as bone graft cement, to accelerate new bone formation is still needed further investigations.

Zeolite is an aluminosilicate material with uniform microporous structure. It has thermal, chemical, and mechanical stabilities and has been used commercially as a catalyst or separation material (9). Zeolite has the

potential for biomedical application due to its non-toxic, antimicrobial and antineoplastic activities and may also serve as a viable carrier, a controlled-release agent and an adjuvant for pharmacotherapy (10-16). Moreover, zeolite coating has been successfully synthesized on the titanium alloy (17,18). This coating is highly corrosion-resistant and has favorable elasticity coefficient (30–40 GPa) similar to that of the bone. Additionally, available studies have indicated the zeolite coating is better to promote adhesion, proliferation and differentiation of cells and has favorable osteoinductive and osteoconductive properties, indicating the highly biocompatibility of this material.

The SiC foam was coated with two types of zeolite (silicalite-1 or ZSM-5) by *in situ* hydrothermal syntheses at the Institute of Metal Research, Chinese Academy of Sciences (Shenyang, China). The present study was to evaluate the biocompatibility of silicalite-1/SiC foam and ZSM-5/SiC foam compared with SiC foam without coating, and further investigate the potential mechanisms underlying these material-induced ossification, which may provide a basis for their use as bone replacement materials.

Methods

Synthesis and morphological observation of silicalite-1/SiC foam and ZSM-5/SiC foam

The SiC foam scaffolds were fabricated by polymer pyrolysis combined with liquid infiltration reaction as previously described (19,20) with following parameters: pore size, 300–1,000 μm; blind hole rate, ≤1%; compression strength, ≥40 MPa; elasticity coefficient, 20–30 GPa. Silicalite-1/SiC foam and ZSM-5/SiC foam scaffolds were produced with the methods reported elsewhere (21). SiC foam was then treated by *in situ* hydrothermal syntheses with a silicon source and an aluminum source at 160 ℃ for 48 h. Subsequently, a nanoscale zeolite coating (25–35 μm thickness) was synthesized on the surface of SiC foam. The samples were molded into cylinder shape sized 11 mm in diameter and 2 mm in height. All the samples were ultrasonically cleaned in acetone, ethanol and distilled water independently, and autoclave-sterilized (121.3 ℃, 103.4 kPa) before cell seeding. The surface morphology of these samples was observed by scanning electron microscopy (SEM, Hitachi S3400N, Japan)

Specific surface area (SSA) and zeta potential of silicalite-1/SiC foam and ZSM-5/SiC foam

The SSA (total surface area/mass, m^2/g) was determined with an automatic micropore and mesopore analyzer (Micromeritics ASAP 2010, USA). The zeta potential of these materials was measured in an aqueous solution (pH 7) with a laser particle analyzer (Nicomp 380 ZLS, USA) at 25 ℃.

Evaluation of biomineralization

The samples were incubated in 25 mL of simulated body fluid (SBF) for 3, 7 or 14 d at a constant temperature (36.5±0.5 ℃). Compositions of bioactive deposits on the surface of these samples were examined by energy dispersive X-ray spectroscopy (EDS).

Protein adsorption assay

Bovine serum albumin (BSA, Glenview, USA) solution at different concentrations (0.05, 0.1, 0.125, 0.2, 0.25, 0.4, 0.5, 0.65, 0.8 and 1 mg/mL) of was prepared to determine the BSA adsorption standard curve. Then, samples were incubated in 50 mL of BSA-phosphate-buffered saline (PBS) solution (1 mg/mL) at a constant temperature (37 ℃) for 5, 10, 20, 30, 45, 60, 90, 120 and 180 min. Subsequently, these samples were removed, and the resultant solution was centrifuged at 12,000 rpm for 5 min at 4 ℃ on a 5430R centrifuge (Eppendorf, Germany). The supernatant was collected, and the protein concentration determined by measuring the UV absorption at 280 nm with a plate reader (Infinite M200, Austria). The amount of BSA adsorbed on these materials was calculated by subtracting the amount of proteins in the solution from the amount of protein added (50 mg).

Culture and identification of primary osteoblasts (authorization number: SCXK LIAO 2008-0005)

All fetal Wistar rats were purchased from the Experimental Animal Centre of China Medical University (Shenyang, China). Rat primary osteoblasts were collected from the femurs and tibias of fetal rats by alternate digestion with trypsin and type I collagen as previously reported (22). Cells were maintained in DMEM supplemented with 10%

FBS (Hyclone, GE Healthcare Life Sciences, Utah, USA) and 1% penicillin/streptomycin (Beyotime, China) in a humidified atmosphere with 5% CO_2 at 37 ℃. These of the third passage were harvested for alkaline phosphatase (ALP) staining, alizarin red staining, and immunofluorescent staining of type I collagen.

Attachment of cells incubated with above samples

Three replicates from uncoated SiC foam, silicalite-1 coated SiC foam or ZSM-5-coated SiC foam samples were placed in 24-well plates (Costar, USA) and then independently incubated in DMEM with 10% FBS for 2 h under sterile conditions. Then, osteoblasts of the fourth to sixth passage were seeded on the materials at a density of 10^5 cells/well, followed by incubation in a humidified environment with 5% CO_2 at 37 ℃ for 3, 5 or 7 d. Thereafter, the samples were rinsed with PBS and fixed in 3% glutaraldehyde buffer for 2 h and in 1% osmic acid for 1 h at 4 ℃. Then, these samples were washed with PBS twice and sequentially treated with 30%, 50%, 70%, 80%, 95% and 100% ethanol for 15 min thrice for each. All the samples were dried at a critical point in the ethanol-amyl acetate mixtures with an increasing ratio (3:1, 1:1, 1:3; 15 min for each) and then in pure amyl acetate for 15 min twice. Subsequently, all the samples were dried in the vacuum. A thin-layer gold was sputter-applied to the surface of these samples before examination under a Hitachi S-3400N scanning electron microscope (Japan). The morphology and adhesion of primary osteoblasts on each type of materials were examined.

Assays of cell proliferation and viability

The proliferation and viability of primary osteoblasts after incubation with SiC foam with or without coating were assessed by the 3-(4,5-dimethylthiazol-2-yl)-2,5-diphenyltetrazolium bromide (MTT) assay. Mitochondrial succinate dehydrogenase in viable cells can convert MTT molecules into blue-purple formazan crystals, which are insoluble. The color intensity is quantified using its corrected absorbance value at 490 nm after the crystals are dissolved in dimethyl sulfoxide (DMSO) and are proportional to the number of viable cells. Materials were incubated with primary osteoblasts at a density of 10^5 cells/well for 1, 3, 5 or 7 d in 24-well plates at 37 ℃ in a humidified incubator with 5% CO_2. At each time point, the culture medium was collected from a well, the latter was rinsed well gently with PBS, and then 40 μL of MTT (5 mg/mL in PBS, Sigma, USA) and 360 μL of DMEM medium without FBS were added into each well. After incubation in an environment with 5% CO_2 at 37 ℃ for 4 h, 200 μL of DMSO (Sigma, USA) was added to dissolve the crystalline particles. The absorbance was measured at 490 nm on a microplate reader (Infinite M200, Austria).

Detection of alkaline phosphate (ALP) activity

This activity of osteoblasts was quantified with the ALP Assay Kit (Jiancheng Biotech, Nanjing, China). After incubation with samples for 1, 3, 5 or 7 d, cells were collected and lysed in 0.3% Triton X-100 with an ultrasonic cell disruptor (Cole-Parmer, USA). Then, 30 μL of cell lysates, 30 μL of 0.02 mg/mL phenol standard solution, or 30 μL of deionized water (blank control) was added into each well in a 96-well plate with 50 μL of substrate solution and 50 μL of buffer in each well, followed by incubation at 37 ℃ for 15 min. Then, the solution for visualization was added (150 μL) into each well. The absorbance was measured at 520 nm on a microplate reader. For normalization, the total protein concentration was determined using the BCA kit (KeyGEN Biotech, China). The ALP concentrations were calculated with following formula:

$$\text{ALP activity}\ (unit/gprot)=\frac{(sample\ OD-blank\ OD)/(phenol\ OD-blank\ OD)\times 0.02\ mg}{total\ protein\ of\ sample\ (mgprot/ml)\times 0.03\ ml}$$

Statistical analysis

All the experiments were repeated at least three times, and data are presented as mean ± standard deviation (SD). One-way analysis of variance (ANOVA) was performed to analyze the difference between groups. Statistical analysis was performed with SPSS version 19.0 package. A value of $P<0.05$ was considered statistically significant.

Results

Surface morphology

Scanning electron microscopy showed SiC foam had polygonal closed-loops as basic units, which formed three-dimensional connected network. On the surface of silicalite-1/SiC foam and ZSM-5/SiC foam, a molecular sieve coating was observed and loaded equably on the ceramic surface of SiC foam. The crystal orientation of molecular sieves distributed randomly, forming a continuous

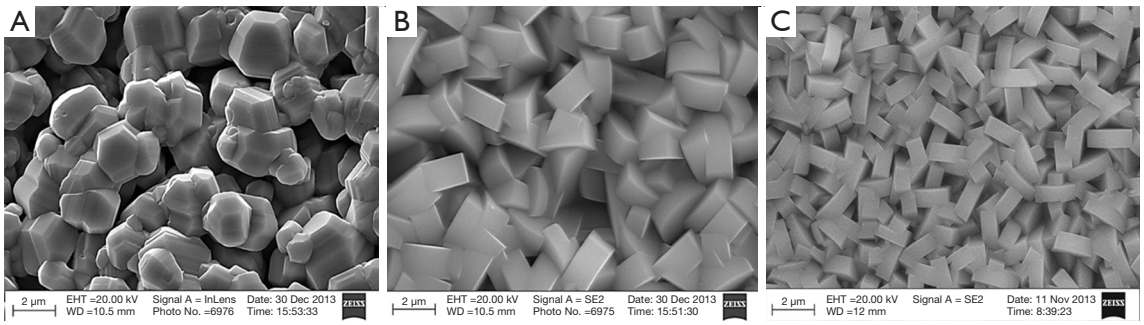

Figure 1 Photographs of SiC foam (A), silicalite-1/SiC foam (B) and ZSM-5/SiC foam (C). SiC, silicon carbide.

Table 1 SSA and zeta potential of different materials

Materials	SSA (m^2/g)	Zeta potential (mV)
SiC foam	0.2±0.01	−18.97±0.94
Silicalite-1/SiC foam	35±2*	−20.52±1.12
ZSM-5/SiC foam	25±1*	−20.05±1.01

*, P<0.001 *vs.* SiC foam. Zeta potential of three types of materials was all negative when pH =7. The zeta potentials of silicalite-1/SiC foam and ZSM-5/SiC foam were slightly higher than that of SiC foam (P>0.05). SSA, specific surface area; SiC, silicon carbide.

coating on the ceramic surface of SiC foam. There were complex three-dimensional cellular structures on the surface of silicalite-1/SiC foam and ZSM-5/SiC foam, which were relatively rough (*Figure 1*).

SSA and zeta potential

The SSA and *zeta* potential of SiC foam, silicalite-1/SiC foam, and ZSM-5/SiC foam are shown in *Table 1*. The SSAs of silicalite-1/SiC foam and ZSM-5/SiC foam were significantly larger than that of SiC foam (P<0.05).

Biomineralization ability

After incubation in SBF for 3 d, no deposits were observed on three materials. A small number of deposits was found on the silicalite-1/SiC foam at 7 d; however, no deposits formed on the ZSM-5/SiC foam and SiC foam at 7 d. After incubation in SBF for 14 d, no deposits were identified on the SiC foam but a small number of deposits formed on the ZSM-5/SiC foam, and a large number of deposits could be found on the silicalite-1/SiC foam (*Figure 2*). EDS analyses indicated the presence of elemental Ca, P, and O in the deposits on the silicalite-1/SiC foam and ZSM-5/SiC foam; these deposits corresponded to an apatite-like layer (*Figure 3*).

Protein adsorption ability

Figure 4 shows a similar trend in the amount of BSA adsorbed on three materials. BSA was quickly adsorbed on the materials in the initial phase, and then this process was slowed down. The adsorption reached the plateau after incubation for approximately 60 min, which suggests that BSA adsorption is a fairly rapid process. Nonetheless, there was significant difference in the amount of BSA adsorbed on three types of materials. The amount of BSA on the silicalite-1/SiC foam or ZSM-5/SiC foam was significantly larger than that on the SiC foam.

Biocompatibility

Culture and identification of primary osteoblasts

Primary osteoblasts after 5 d culture mainly had triangular or spindle shape and were closely connected (*Figure 5A*). The ALP staining revealed typical dual nuclei in osteoblasts, and the cytoplasm was dark blue (*Figure 5B*). Alizarin red staining showed calcium nodes were red (*Figure 5C*). Type I collagen immunofluorescent staining indicated the cytoplasm was red, and the nucleus stained with 4',6-diamidino-2-phenylindole (DAPI) was blue (*Figure 5D*).

Cell attachment

After incubation with SiC foam, silicalite-1/SiC foam or ZSM-5/SiC foam for 3, 5 or 7 d, scanning electron microscopy revealed primary osteoblasts were adherent to the samples (*Figure 6*). In the early stage of adhesion, the osteoblasts were small and insular, with rough and scraggly

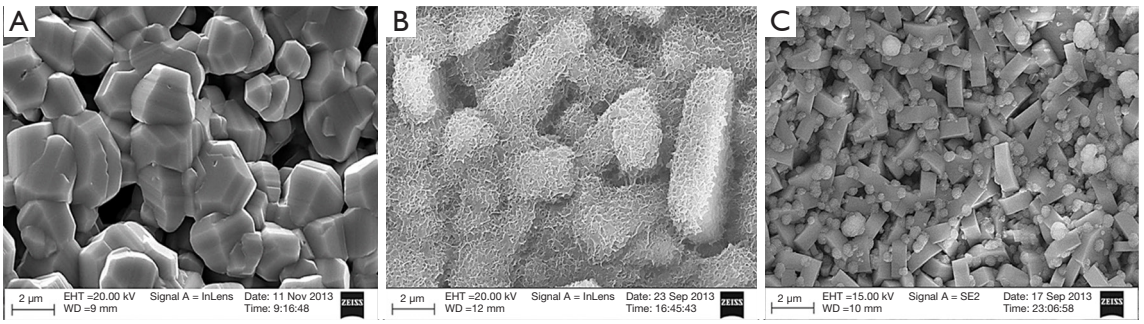

Figure 2 Mineralization on three materials observed with a scanning electron microscope at 14 days. No deposits were observed on SiC foam (A); mineralization deposits were found on silicalite-1/SiC foam (B) and ZSM-5/SiC foam (C). SiC, silicon carbide.

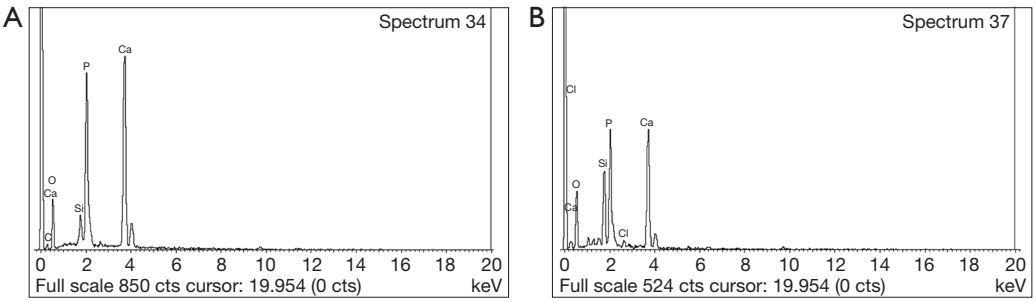

Figure 3 EDS analysis of deposits on silicalite-1/SiC foam (A) and ZSM-5/SiC foam (B). The Ca, P and O elements were identified in the deposits on silicalite-1 and ZSM-5/SiC foam, which corresponded to an apatite-like layer. EDS, energy dispersive X-ray spectroscopy; SiC, silicon carbide.

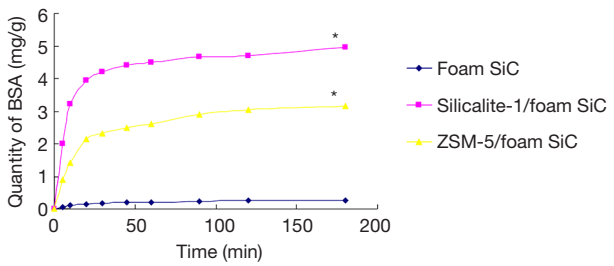

Figure 4 BSA adsorbed on three materials. BSA was quickly adsorbed on the materials in initial phase and then the absorption was gradually slowed down. Adsorption equilibrium reached the plateau after incubation for approximately 60 min. The amount of BSA absorbed on silicalite-1 and ZSM-5/SiC foam was larger than that on SiC. *, P<0.05 *vs.* SiC foam. BSA, bovine serum albumin; SiC, silicon carbide.

spindle-like, triangular or polygonal shape. The number and volume of cells increased, cytoplasm expansion was notable, and cell borders became blur over time. Osteoblasts formed long spindles or flat polygons and maintained physical contact through pseudopodia. The attachment of primary osteoblasts incubated with different materials was similar and there was no evidence on major deleterious or cytotoxic effects.

Cell proliferation and activity

As shown in *Figure* 7, the proliferation of cells incubated with different materials continued to increase over time. The proliferation of cells incubated with silicalite-1/SiC foam and ZSM-5/SiC foam was higher than that of cells incubated with SiC foam at each time point, and significant difference was noted at 5 and 7 d (P<0.05). Moreover, there was marked difference between silicalite-1/SiC foam and ZSM-5/SiC foam groups (P>0.05). These results indicate silicalite-1/SiC foam and ZSM-5/SiC foam have no cytotoxic effects on primary osteoblasts. These cells can proliferate faster on the zeolite-coated surfaces than on SiC foam, indicating higher proliferation promoting capability of the silicalite-1/SiC foam and ZSM-5/SiC foam.

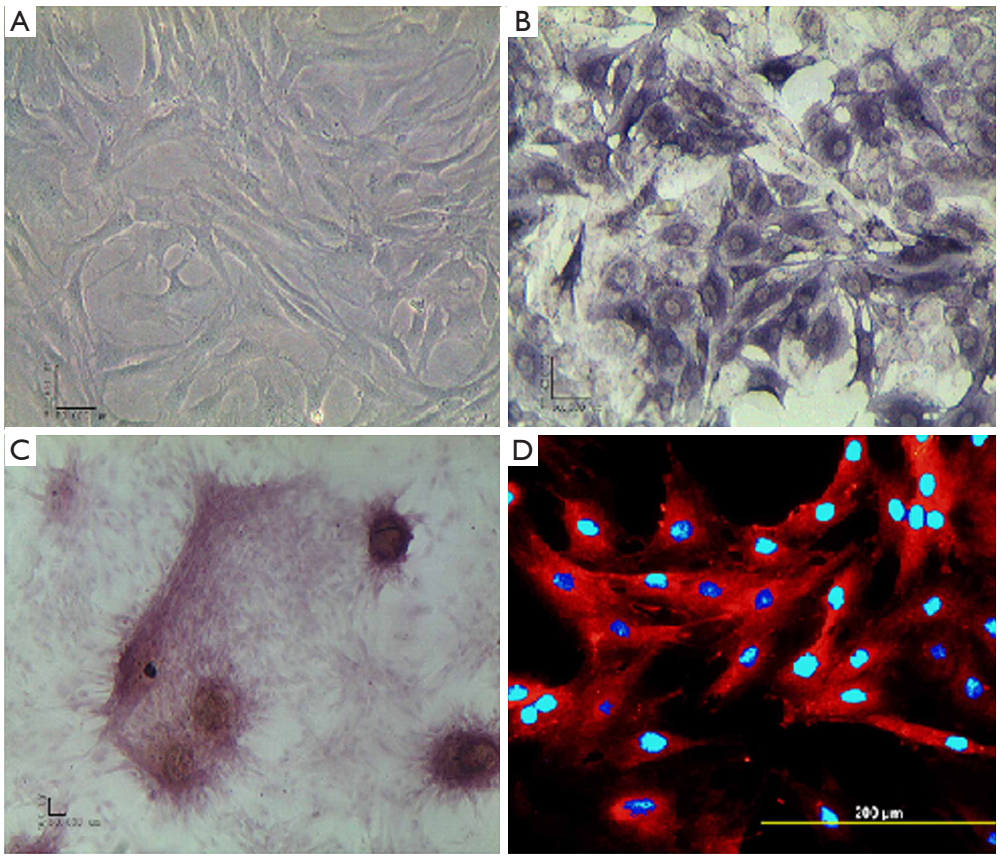

Figure 5 Primary osteoblasts after staining: (A) primary osteoblasts without staining, (B) ALP staining, (C) alizarin red staining, (D) collagen I immunofluorescence staining. Scale bar =200 μm. ALP, alkaline phosphatase.

Cell differentiation

The ALP activity was 8.16±0.40 units/gprot for SiC foam, 8.91±0.44 units/gprot for silicalite-1/SiC foam and 8.45±0.42 units/gprot for ZSM-5/SiC foam at 1 d, and it increased to 13.81±0.69 units/gprot for SiC foam, 16.26±0.81 units/gprot for silicalite-1/SiC foam and 16.24±0.81 units/gprot for ZSM-5/SiC foam at 7 d. There was significant difference in the ALP activity between silicalite-1/SiC foam/ZSM-5/SiC foam and SiC foam at 7 d ($P<0.05$). The ALP activity was comparable between silicalite-1/SiC foam group and ZSM-5/SiC foam group at each time point ($P>0.05$; *Figure 8*).

Discussion

Our previous study compared the biocompatibility between uncoated SiC foam and porous HA and revealed that SiC foam had comparable influences or long-term effects on the adhesion, proliferation and differentiation capacities of primary osteoblasts (8). This study aimed to investigate the bioactivity and *in vitro* biocompatibility of SiC foam coated with one of two types of zeolite (silicalite-1 or ZSM-5) as compared to uncoated SiC foam.

Studies (23,24) have shown that bioactive glasses and bioceramics are osseointegrated because bone like apatite can be formed on these materials after implantation, significantly promote osteoblast adhesion and proliferation and accelerate new bone formation and growth. In our study, the bioactivity of silicalite-1/SiC foam and ZSM-5/SiC foam) was assessed *in vitro*. EDS analyses indicated the presence of Ca, P, and O in the deposits on silicalite-1/SiC foam and ZSM-5/SiC foam; these deposits corresponded to an apatite-like layer. These suggest that both silicalite-1/SiC foam and ZSM-5/SiC foam have better bioactivity than SiC foam does. The formation of bonelike apatite is the process of formation and growth of bones. The zeta potential measurements showed silicalite-1/SiC foam and ZSM-5/SiC foam had more negative surface charges as compared

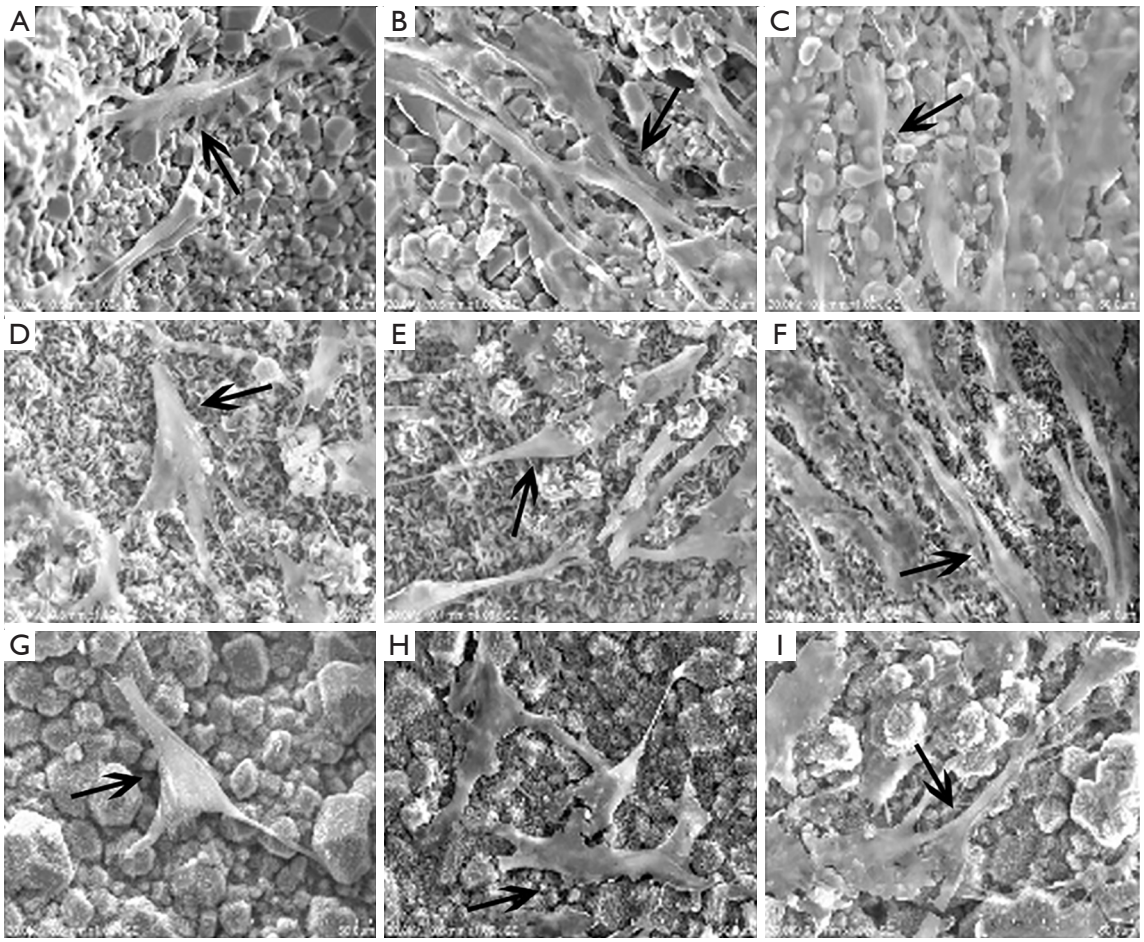

Figure 6 The primary osteoblasts on SiC foam (A,B,C), silicalite-1/SiC foam (D,E,F), and ZSM-5/ SiC foam (G,H,I) at 3 d (A,D,G), 5 d (B,E,H) and 7 d (C,F,I) (scanning electron microscopy). Magnification: 1,000×. Arrow: osteoblasts.

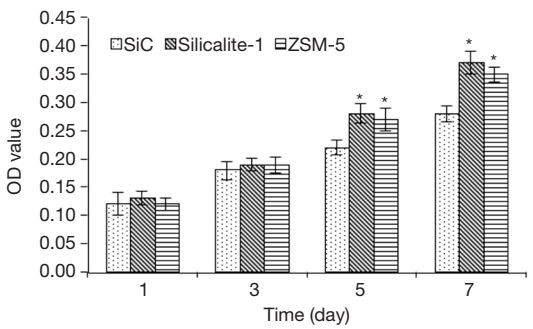

Figure 7 MTT assay of cell proliferation. The proliferation of cells on silicalite-1/SiC foam and ZSM-5/SiC foam was higher than that on SiC foam at each time point, and significant difference was observed at 5 d and 7 d (*, P<0.05 *vs.* SiC foam). MTT, 3-(4,5-dimethylthiazol-2-yl)-2,5-diphenyltetrazolium bromide; SiC, silicon carbide.

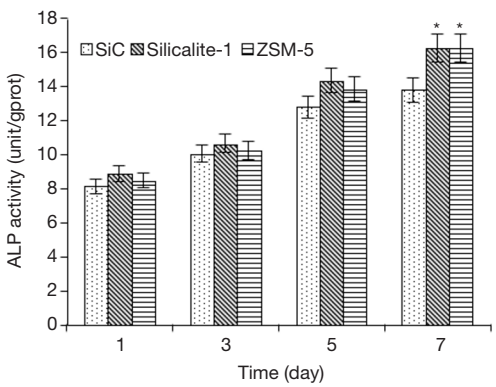

Figure 8 ALP activity of SiC scaffolds at 1, 3, 5 and 7 d. There was a significant difference in the ALP activity between silicalite-1/SiC foam/ZSM-5/SiC foam and SiC foam at 7 d (*, P<0.05 *vs.* SiC foam). ALP, alkaline phosphatase; SiC, silicon carbide.

to SiC foam. Negative surface charges are more likely to interact with cations such as Ca^{2+} and P^{3+} in solution to form amorphous or nanocrystalline calcium phosphate, which carries a positive surface charge. Then, they attract anionic groups (such as PO_4^{3-}). With the increase in local oversaturation, calcium and phosphorus nucleation occurs, crystals gradually grow, and finally a bone-like apatite layer forms. These results are in agreement with other reports (25). Also, silicalite-1/SiC foam and ZSM-5/SiC foam have a larger SSA, providing more adhesion sites for Ca^{2+} and P^{5+}, which is better for biomineralization (26).

Biomaterials interact with proteins when they contact with blood and interstitial fluid after implantation. The adsorbed proteins play a significant role in subsequent cell behaviors and have important influences on the final implantation (27,28). The amount of BSA absorbed on silicalite-1/SiC foam and ZSM-5/SiC foam was larger than that on SiC foam, suggesting better bioactivity. These may be related to the larger SSAs of silicalite-1/SiC foam and ZSM-5/SiC foam, thus providing more adhesion sites for BSA adsorption.

Stronger adhesion, greater proliferation and differentiation of osteoblasts were observed after incubation with silicalite-1/SiC foam and ZSM-5/SiC foam as compared to SiC foam. These may be attributed to the uniform three-dimensional microporous structure provided by the zeolite crystals, with nanometer-scale pores (0.3–2.0 nm usually) and a complicated microcrystal topology, which offers larger SSA and more attachment sites for osteoblast adhesion, proliferation, and differentiation (29-32). In addition, more negative surface charges ensure the collection and adsorption of cations such as Ca^{2+} and proteins (33), thus promoting cell adhesion and proliferation.

In conclusion, the biocompatibility of silicalite-1/SiC foam and ZSM-5/SiC foam method was evaluated in the present study. Silicalite-1/SiC foam and ZSM-5/SiC foam have favorable biocompatibility and no cytotoxic effect on primary osteoblasts; therefore, both are helpful for the adhesion, proliferation, and differentiation of primary osteoblasts and have the potential to serve as new bone replacement materials.

Acknowledgments

We thank Professor Jinsong Zhang at the Institute of Metal Research for his support with the materials. We thank Li Zhu at the Experiment Centre of the School of Stomatology, China Medical University, for her support of cell culture.

Funding: The study was supported by the Science and Technology Project of Liaoning Province, China (No. 2013225090).

Footnote

Conflicts of Interest: The authors have no conflicts of interest to declare.

References

1. Lasanianos N, Kanakaris N, Giannoudis P. Current management of long bone large segmental defects. Orthop Trauma 2010;24:149-63.
2. Diaz-Rodriguez P, Landin M. Biomorphic Ceramics for Drug Delivery in Bone Tissue Regeneration. Curr Pharm Des 2017;23:3507-14.
3. Gryshkov O, Klyui NI, Temchenko VP, et al. Porous biomorphic silicon carbide ceramics coated with hydroxyapatite as prospective materials for bone implants. Mater Sci Eng C Mater Biol Appl 2016;68:143-52.
4. Lopa S, De Girolamo L, Arrigoni E, et al. Enhanced biological performance of human adipose-derived stem cells cultured on titanium-based biomaterials and silicon carbide sheets for orthopaedic applications. J Biol Regul Homeost Agents 2011;25:S35-42.
5. Oliveros A, Guiseppi-Elie A, Saddow SE. Silicon carbide: a versatile material for biosensor applications. Biomed Microdevices 2013;15:353-68.
6. Wu L, Xu X, Li B, et al. Biocompatibility of silicon carbide foam. Chin J Mater Res 2008;22:58-62.
7. Wu L, Xu XX, Wang LZ, et al. Study on cytocompatability and animal implantation test of foam SiC. J Inorganic Materials 2010;25:211-5.
8. Wu L, Yuan Y, Hao FY. The effects of SiC foams on cell proliferation and differentiation in primary osteoblasts. J Hard Tissue Biol 2015;24:37-42.
9. Balkus KJ Jr, Gabrielov AG. Zeolite encapsulated metal complexes. J Incl Phenom Mol Recog Chem 1995;21:159-84.
10. Domingo C, García-Carmona J, Fanovich MA, et al. Study of adsorption processes of model drugs at supercritical conditions using partial least squares regression. Anal Chim Acta 2002;452:311-9.
11. Dyer A, Morgan S, Wells P, et al. The use of zeolites as slow release anthelmintic carriers. J Helminthol 2000;74:137-41.

12. Fox S, Wilkinson TS, Wheatley PS, et al. NO-loaded Zn(2+)-exchanged zeolite materials: a potential bifunctional anti-bacterial strategy. Acta Biomater 2010;6:1515-21.
13. Jung BG, Toan NT, Cho SJ, et al. Dietary aluminosilicate supplement enhances immune activity in mice and reinforces clearance of porcine circovirus type 2 in experimentally infected pigs. Vet Microbiol 2010;143:117-25.
14. Katic M, Bosnjak B, Gall-Troselj K, et al. A clinoptilolite effect on cell media and the consequent effects on tumor cells in vitro. Front Biosci 2006;11:1722-32.
15. Pavelić K, Hadzija M, Bedrica L, et al. Natural zeolite clinoptilolite: new adjuvant in anticancer therapy. J Mol Med (Berl) 2001;78:708-20.
16. Yang P, Quan Z, Li C, et al. Bioactive, luminescent and mesoporous europium-doped hydroxyapatite as a drug carrier. Biomaterials 2008;29:4341-7.
17. Bedi RS, Beving DE, Zanello LP, et al. Biocompatibility of corrosion-resistant zeolite coatings for titanium alloy biomedical implants. Acta Biomater 2009;5:3265-71.
18. Bedi RS, Zanello LP, Yan Y. Osteoconductive and Osteoinductive Properties of Zeolite MFI Coatings on Titanium Alloys. Adv Funct Mater 2010;19:3856-61.
19. Tian C, Zhang JS, Cao XM, et al. High strength silicon carbide foams and their deformation behavior. J Mater Sci Technol 2006;22:269-72.
20. Zhang JS, Cao XM. Compact foamed thyrite with high intensity and preparation method of the same. World Patent 2007:WO2007056895.
21. Jiao YL, Yang ZM, Cao XM, et al. In situ synthesis of silicalite-1 type zeolite on SiC foam ceramics. Rare Metal Mat Eng 2009;38:286-8.
22. Yuan Y, Si-Dalai HA, Zhu HT, et al. Primary culture of osteoblasts from fetal rat. Chin J Pract Stomatol 2010;3:607-9.
23. El-Ghannam A, Ducheyne P, Shapiro IM. Effect of serum proteins on osteoblast adhesion to surface-modified bioactive glass and hydroxyapatite. J Orthop Res 1999;17:340-5.
24. Loty C, Sautier JM, Boulekbache H, et al. In vitro bone formation on a bone-like apatite layer prepared by a biomimetic process on a bioactive glass-ceramic. J Biomed Mater Res 2000;49:423-34.
25. Kim HM, Himeno T, Kokubo T, et al. Process and kinetics of bonelike apatite formation on sintered hydroxyapatite in a simulated body fluid. Biomaterials 2005;26:4366-73.
26. Le Guéhennec L, Soueidan A, Layrolle P, et al. Surface treatments of titanium dental implants for rapid osseointegration. Dent Mater 2007;23:844-54.
27. Kaufmann EA, Ducheyne P, Radin S, et al. Initial events at the bioactive glass surface in contact with protein-containing solutions. J Biomed Mater Res 2000;52:825-30.
28. Puleo DA, Nanci A. Understanding and controlling the bone-implant interface. Biomaterials 1999;20:2311-21.
29. Balasundaram G, Webster TJ. A Perspective on Nanophase Materials for Orthopaedic Implant Applications. J Mater Chem 2006;16:3737-45.
30. Feng B, Weng J, Qu S, et al. Nano-structuralized surface modification for biomedical titanium. Rare Metal Mat Eng 2007;36:1693-7.
31. Popat KC, Leoni L, Grimes CA, et al. Influence of engineered titania nanotubular surfaces on bone cells. Biomaterials 2007;28:3188-97.
32. Setzer B, Bachle M, Metzger MC, et al. The gene-expression and phenotypic response of hFOB 1.19 osteoblasts to surface-modified titanium and zirconia. Biomaterials 2009;30:979-90.
33. Bodhak S, Bose S, Bandyopadhyay A. Role of surface charge and wettability on early stage mineralization and bone cell-materials interactions of polarized hydroxyapatite. Acta Biomater 2009;5:2178-88.

Cite this article as: Hao F, Zhang C, Wu L, Gao Y, Jiao Y. Both silicalite-1/SiC foam and ZSM-5/SiC foam may serve as novel bone replacement materials. Ann Transl Med 2019;7(12):255. doi: 10.21037/atm.2019.05.06

